Nonlinear analysis of stationary patterns in convection-reaction-diffusion systems

Olga A. Nekhamkina,[1] Alexander A. Nepomnyashchy,[2,3] Boris Y. Rubinstein,[1,3] and Moshe Sheintuch[1,3]

[1]*Department of Chemical Engineering, Technion–IIT, Technion City, Haifa 32 000, Israel*
[2]*Department of Mathematics, Technion–IIT, Technion City, Haifa 32 000, Isreal*
[3]*Minerva Center for Research in Nonlinear Phenomena, Technion–IIT, Technion City, Haifa 32 000, Israel*

Stationary spatially inhomogeneous patterns which appear due to the interaction of reaction and convection in a packed-bed cross-flow reactor are observed and analyzed. A linear stability analysis was performed for the case of unbounded system, and an analytical expression for the amplification threshold was determined. Above this threshold stationary patterns could be sustained in bounded systems. A weakly nonlinear analysis is used in order to derive the governing amplitude equation. The results of linear and nonlinear analyses were verified by direct numerical simulations.

PACS number(s): 82.40.Ck, 47.54.+r

I. INTRODUCTION

In this work we describe the emergence of stationary patterns due to interaction of convection, conduction (or diffusion), and reaction in a realistic model of a catalytic membrane reactor. Aside from describing the phenomena we aim to derive a general complex Ginzburg-Landau (CGL)-like model. While such models that account for both diffusion and convection have been studied by several groups, we highlight the importance of boundary conditions for pattern selection, and point to the problem of translating real boundary conditions to those of the CGL model. It was demonstrated in several studies that pattern selection in a bounded region is significantly affected by the boundary conditions. Deissler [1] was probably the first to point out the important role of boundary conditions, but he was interested mainly in the effect of boundaries as a source through which disturbances are injected into the flow and propagate downstream. In subsequent works [2–4] the effect of various types of boundary conditions including reflective and absorbing boundaries was investigated using the CGL equation. It was established that close to threshold the dynamics of a bounded system is reasonably well described by the amplitude equation derived for the infinite system [5].

Spatiotemporal patterns in reaction-diffusion systems have been studied extensively, and typically emerge due to the interaction of a short-range activator with a highly diffusing inhibitor. Oscillations in high- and low-pressure catalytic systems are accounted for by a fast activator and a slow but localized (nondiffusing) inhibitor. Typically, the fast set in catalytic reactors accounts for reactant concentration and the catalyst temperature, while the slow inhibitor is the catalytic activity, as described above. The identity and the kinetics of the latter are still debated. Patterns in such systems may emerge due to long-range interaction imposed by global control or by gas-phase mixing and were recently studied by our group as well as other groups (see the review by Sheintuch and Schvartsman [6]). When the activity is fixed the system decays into a steady state due to the large heat capacity of the catalyst. The model considered here assumes a fixed activity, and patterns emerge due to the interaction of convection and reaction.

Commercial catalytic reactors are typically organized as packed beds with the flow of the reactants and products through the bed of catalytic pellets. Pattern formation in convection-conduction-reaction systems with a simple exothermic and activated catalytic reaction has recently attracted considerable attention. Convection will affect the emerging patterns in oscillatory systems, as demonstrated in recent studies [7]. A reactor with flow reversal was extensively studied and installed commercially [8]. Patterns due to front feedback in a loop reactor were recently demonstrated by Gilles and co-workers in Refs. [9,10].

We consider a membrane (or cross-flow) reactor with realistic parameters [high heat capacity and small axial dispersion (diffusion)]: physically it requires a continuous supply of reactants along the bed, so that a homogeneous (space-independent) solution may be attained. A similar model was used in recent works by Yakhnin and co-workers [11–13] devoted to differential flow induced chemical instability in a one-dimensional tubular cross-flow reactor. Linear stability analysis around a spatially homogeneous solution was used to obtain the dispersion relation, and some useful estimations of the possible wave numbers were obtained. The patterns excited above the convective instability threshold are washed out in bounded system, so the authors used temporal forcing at the reactor inlet in order to excite nonvanishing inhomogeneous structures. It should be underlined that these patterns are periodic in time, and characterized by a nonzero amplitude growth rate.

In the model discussed below we consider two types of boundary conditions—periodic, and realistic Danckwert's type. For the former type we found well known travelling wave solutions described by a complex Ginzburg-Landau equation. For the latter the homogeneous state typically does not satisfy the boundary conditions, and the emerging inhomogeneous structure is not the result of the bifurcation but can be viewed as the system response to the boundary conditions.

The structure of this work is as follows. The reactor model in both dimensional and dimensionless forms is introduced in Sec. II. In Sec. III a neutral curve for an unbounded system with a minimum corresponding to an oscillatory (Hopf) bifurcation is obtained by means of linear analysis. This minimum represents the convective instability threshold. Periodic boundary conditions may lead to a shift of the

critical wave number, but the type of bifurcation is preserved. It is shown that the phase velocity is not constant along the neutral curve; moreover, it may change its sign at some point on the curve. This point corresponds to the amplification threshold, so that it appears to be very important for further analysis of the system. In a semi-infinite region or a finite region, traveling waves decay if the instability is convective. Danckwert's boundary conditions produce a certain stationary regime instead of traveling waves. Its properties are essentially different below and above the amplification threshold. Only after the amplification threshold is passed does one obtain new patterns.

The nonlinear analysis is performed in Sec. IV and the governing equation for a perturbation amplitude is derived. For periodic boundary conditions the result is quite standard [it leads to the complex Ginzburg-Landau equation (CGLE)], and it is not presented. In the vicinity of the amplification threshold, in contrast to the standard CGLE, the governing amplitude equation lacks the diffusional term, while the convective term is present, and the latter have a complex (velocity) coefficient. The cases where this equation is well posed are found and discussed.

The stability analysis results are checked against direct numerical simulations presented in Sec. V. They confirm the excitation of traveling waves in a system with periodic boundary conditions, and the decay of these solutions for realistic boundary conditions below the amplification threshold. Numerics also show that above this threshold stationary structures emerge, these patterns remain stable even far from threshold, while the profile changes significantly. Note that the developed theory is valid if the critical wavelength is significantly smaller than the size of the system.

II. REACTOR MODEL

Consider the main physical phenomena that take place in a one-dimensional membrane (or cross-flow) reactor in which a first-order exothermic reaction occurs. By membrane reactors we imply a fixed bed, in which the reactants flow and react, while a small stream of highly concentrated reactants is supplied continuously (by diffusion or flow) through the reactor wall. Dispersion of a reactant along a packed-bed reactor, rather than supplying it with the feed, may be advantageous in several classes of reactions (see the discussion in Ref. [14]). A continuous supply of a reactant may also be effectively achieved in a sequence of two consecutive reactions, when the first one is reacts at an almost constant rate. The mathematical model accounts for the fast and localized concentration C and the slow and conducting temperature T, which can also be viewed as the activator. The mass and energy balances are conventional ones except for the mass supply term; they account for accumulation, convection, axial dispersion, chemical reaction $r(C,T)$, heat loss due to cooling $[S_T = \alpha_T(T - T_w)]$, and mass supply through a membrane wall $[S_C = \alpha_C(C - C_w)]$. For the one-dimensional case the appropriate system of equations has the following forms:

$$\frac{\partial C}{\partial t} + u\frac{\partial C}{\partial z} - \epsilon D_f\frac{\partial^2 C}{\partial z^2} = -(1-\epsilon)r(C,T) + S_C,$$

(1)

$$(\rho c_p)_e\frac{\partial T}{\partial t} + (\rho c_p)_f u\frac{\partial T}{\partial z} - k_e\frac{\partial^2 T}{\partial z^2}$$

$$= (-\Delta H)(1-\epsilon)r(C,T) + S_T.$$

Danckwert's boundary conditions are typically imposed on the model:

$$z=0, \quad \epsilon D_f\frac{\partial C}{\partial z} = u(C - C_{in}), \quad k_e\frac{\partial T}{\partial z} = (\rho c_p)_f u(T - T_{in});$$

(2)

$$z=L, \quad \frac{\partial T}{\partial z} = \frac{\partial C}{\partial z} = 0.$$

Mass dispersion is typically negligible. A first-order activated kinetics $r = A\exp(-E/RT)C$ is assumed. The appropriate mathematical model may be written in the dimensionless form of Eqs. (1) and (2) (see Ref. [7] for a derivation):

$$\frac{\partial x}{\partial \tau} + \frac{\partial x}{\partial \xi} = (1-x)G(y) - (x - x_w) = f(x,y),$$

$$\text{Le}\frac{\partial y}{\partial \tau} + \frac{\partial y}{\partial \xi} - \frac{1}{\text{Pe}}\frac{\partial^2 y}{\partial \xi^2} = B(1-x)G(y) - \alpha(y - y_w) = g(x,y),$$

(3)

$$G(y) = \text{Da}\exp\left(\frac{\gamma y}{\gamma + y}\right).$$

First Eqs. (3) will be treated in an unbounded region. Although this solution can hardly be realized, technically it provides some insight into the bounded system case. Later we supply it with Danckwert's boundary conditions

$$\xi=0, \quad x=x_{in}, \quad \frac{\partial y}{\partial \xi} = \text{Pe}(y - y_{in}), \quad \xi = \xi_{ex}, \quad \frac{\partial y}{\partial \xi} = 0.$$

(4)

Here the dependent variables are normalized in a standard way, but independent variables and nondimensional parameters (Da, Pe) are normalized with respect to the mass transfer coefficient α_c:

$$x = \frac{C_{in} - C}{C_{in}}, \quad y = \gamma\frac{T - T_{in}}{T_{in}}, \quad \xi = \frac{\alpha_C z}{L}, \quad \tau = \frac{\alpha_C t u}{L},$$

$$\gamma = \frac{E}{RT_{in}}, \quad B = \gamma\frac{(-\Delta H)C_{in}}{(\rho c_p)_f T_{in}}, \quad \text{Le} = \frac{(1-\epsilon)(\rho c_p)_s}{(\rho c_p)_f},$$

(5)

$$\text{Pe} = \frac{(\rho c_p)_f L u}{k_e \alpha_C}, \quad \text{Da} = \frac{AL}{u\alpha_C}e^{-\gamma},$$

$$\alpha_C = \frac{k_g PL}{u}, \quad \alpha = \frac{h_T PL}{(\rho c_p)_f u\alpha_C}.$$

In order to reduce the number of free parameters we used $T_w = T_{in}$, i.e., $y_{in} = y_w = 0$; note that $x_w < 0$ corresponds to the case $C_w > C_{in}$. The length of the reactor ξ_{ex} was chosen to resolve the structure of emerging patterns.

III. LINEAR ANALYSIS

System (3) in an unbounded region may admit multiple homogeneous solutions x_s and y_s of the corresponding algebraic system $f(x,y)=g(x,y)=0$. The roots x_s and y_s are linearly dependent, and the y_s values may be determined from the equation

$$H(y_s)G(y_s)=\alpha(y_s-y_w),\qquad(6)$$

where

$$H(y_s)=B(1-x_w)-\alpha(y_s-y_w).$$

The left hand side of Eq. (6) is a ''sigmoidal curve,'' and up to three intersections with the straight line [the right hand side of Eq. (6)] may exist. The multiplicity of the homogeneous solutions as well as the dynamic behavior of the related system

$$\frac{\partial x}{\partial \tau}=f(x,y),\quad \frac{\partial y}{\partial \tau}=g(x,y)\qquad(7)$$

was extensively investigated in Refs. [15,16], as it describes the temporal dynamics of a continuously stirred tank reactor (CSTR). This problem can exhibit a plethora of phase plane regimes, including a simple limit cycle, a pair of stable and unstable limit cycles around a stable state, the coexistence of a limit cycle with a low-conversion stable state, and a limit cycle surrounding three unstable states. We expect that the spatiotemporal behavior of the distributed system (3) is related to the corresponding CSTR problem. Obviously, in the limit of large Peclet numbers Pe$\rightarrow\infty$, the steady state solutions of Eq. (3), if they exist, are fully equivalent to the temporal solution of Eq. (7) (with ξ instead of τ). However, a comprehensive investigation of the behavior of system (3) is beyond the limits of this study. We shall consider a particular case when system (3) admits three homogeneous solutions; the results presented below are obtained only for the upper one. Other situations are considered elsewhere [17].

The stability of the solution (x_s,y_s) can be determined by means of a linear stability analysis. Denoting deviations from the basic solution as (x_1,y_1), and linearizing the original problem, we arrive at the following system for the disturbances:

$$\frac{\partial x_1}{\partial \tau}=-\frac{\partial x_1}{\partial \xi}-(1+G(y_s))x_1+G'(y_s)\frac{H(y_s)}{B}y_1,$$

$$(8)$$

$$\frac{\partial y_1}{\partial \tau}=-\text{Le}^{-1}\frac{\partial y_1}{\partial \xi}+\frac{1}{\text{Le Pe}}\frac{\partial^2 y_1}{\partial \xi^2}$$

$$-\frac{B}{\text{Le}}G(y_s)x_1+G'(y_s)\frac{H(y_s)}{\text{Le}}y_1-\frac{\alpha}{\text{Le}}y_1.$$

Assuming disturbances to be harmonic in the space variable ξ, i.e., $(x_1,y_1)\sim e^{ik\xi+\sigma t}$, where k is the disturbance wave number and σ is its growth rate, and using it in Eq. (9), we arrive at the dispersion relation $\mathcal{D}(\sigma,k)=0$. This has form of a quadratic equation with *complex* coefficients,

$$\sigma^2+(A_r+iA_i)\sigma+(N_r+iN_i)=0,\qquad(9)$$
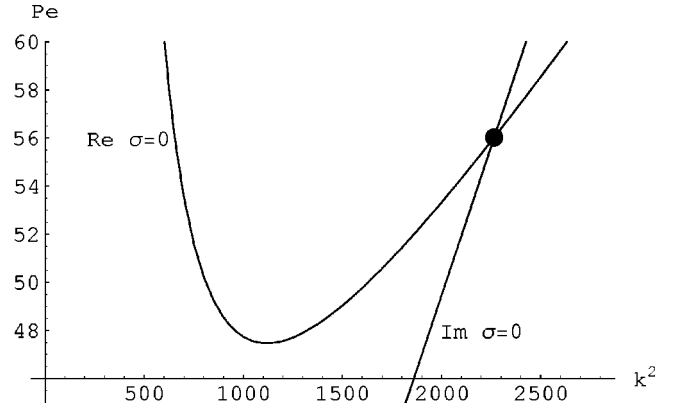
FIG. 1. The neutral curve determined by relation (11) calculated with $B=30$, $\gamma=20$, $\alpha=20$, $x_w=-11$, $y_w=0$, and Le$=333$; the value of Da corresponds to the upper branch of the basic solution $y_s=17.54$. The dot on the curve corresponds to the amplification threshold.

where the coefficients are determined by the following formulas:

$$A_r=1+G(y_s)+\frac{k^2+\alpha\,\text{Pe}}{\text{Le Pe}}-G'(y_s)\frac{H(y_s)}{\text{Le}},\quad A_i=k\frac{1+\text{Le}}{\text{Le}},$$

$$N_r=-G'(y_s)\frac{H(y_s)}{\text{Le}}+k^2\frac{1+G(y_s)-Pe}{\text{Le Pe}}+\frac{\alpha(1+G(y_s))}{\text{Le}},$$

$$(10)$$

$$N_i=-kG'(y_s)\frac{H(y_s)}{\text{Le}}+k\frac{1+\alpha+G(y_s)}{\text{Le}}+\frac{k^3}{\text{Le Pe}}.$$

It can be easily shown that the bifurcation condition Reσ $=0$ is satisfied if

$$A_r^2 N_r+A_r A_i N_i=N_i^2,\qquad(11)$$

while the frequency of the emerging oscillatory pattern is given by

$$\omega_c=\text{Im}\,\sigma=-N_i/A_r.\qquad(12)$$

The latter should be calculated at the point corresponding to the minimum of the neutral curve determined by relation (11). This curve can be found numerically, and typically acquires the form shown in Fig. 1 (the chosen bifurcation parameter is Pe).

The minimum of the curve (k_c,Pe_c) corresponds, in an unbounded system, to the excitation of moving waves. For bounded system with periodic boundary conditions the critical wave number value may be shifted. On the other hand, this minimum coincides with the threshold of the convective instability; hence any spatial nonuniformities are advected in the direction determined by the sign of the phase velocity $(d\omega/dk)_c$, and in the finite region these disturbances can survive only for periodic boundary conditions. In a finite region with realistic boundary conditions these perturbations would inevitably decay.

Because our main goal is to study the influence of stationary nonhomogeneous boundary conditions, we will also investigate the transition between nontransparency and ampli-

fication for stationary boundary disturbances [18]. We have shown that this transition is connected with a point on the neutral curve corresponding to the zero wave velocity. The location of this point is determined by Eq. (11) supplemented by a condition of zero frequency $N_i = 0$ shown by the line $\mathrm{Im}\,\sigma = 0$. This additional condition determines a point at the neutral curve which is shown in Fig. 1; its location is determined as follows:

$$k_0 = [G(y_s)G'(y_s)H(y_s) - (1 + G(y_s))^2]^{1/2},$$

$$\mathrm{Pe}_0 = -\frac{k_0^2}{1 + \alpha + G(y_s) - G'(y_s)H(y_s)}.$$

(13)

At this point the imaginary part of some complex root k of the dispersion relation $\mathcal{D}(\sigma, k) = 0$ tends to zero at $\sigma \to 0$. The value $\mathrm{Pe} = \mathrm{Pe}_0$ corresponds to the transition from nontransparency to amplification regime (see Ref. [18]).

IV. NONLINEAR ANALYSIS

In order to investigate the spatial decay (in the nontransparency region) and the nonlinear spatial growth (in the amplification region) of a stationary boundary disturbance near the point $\mathrm{Pe} = \mathrm{Pe}_0$, we will develop an appropriate amplitude equation which is valid near that point and describes just the amplified and weakly decaying disturbances, i.e., disturbances with k near k_0.

A. Derivation of the amplitude equation

The nonlinear analysis is made by means of the multiscale expansion approach [19]. In this section we sketch major steps of derivation of amplitude equation for the unbounded system under investigation.

We introduce a hierarchy of time scales,

$$\partial/\partial t = \partial/\partial t_0 + \epsilon \partial/\partial t_1 + \epsilon^2 \partial/\partial t_2 + \cdots, \quad (14)$$

and expand in Taylor series the phase variables and the bifurcation parameter,

$$\mathbf{u} = \mathbf{u}_0 + \epsilon \mathbf{u}_1 + \epsilon^2 \mathbf{u}_2 + \cdots, \quad \mathrm{Pe} = \mathrm{Pe}_0 + \epsilon \mathrm{Pe}_1 + \epsilon^2 \mathrm{Pe}_2 + \cdots, \quad (15)$$

where $\mathbf{u} = \{x, y\}$. We also determine two spatial scales:

$$\partial/\partial \xi = \partial/\partial \xi_0 + \epsilon^\beta \partial/\partial \xi_1; \quad (16)$$

here the value of β should be chosen to balance terms of different orders of ϵ properly.

In the case of the Hopf bifurcation with the critical point located at the minimum of the neutral curve, the spatial scaling β is half that of the bifurcation parameter deviation (which usually is set equal to 2, i.e., $\mathrm{Pe}_1 = 0$). The derivation of the amplitude equation in this case is quite standard, resulting in the CGLE. The solution of this equation determines an amplitude of the traveling waves excited above the bifurcation threshold. Numerical simulations shows that this equation describes the emerging nonstationary patterns quite well (see Sec. V). In the case with $\mathrm{Im}\,\sigma = 0$ the point (k_0, Pe_0) is usually located at the linear section of the neutral

curve, and the bifurcation parameter deviation should be of the same order of magnitude as the spatial scaling β, so $\beta = 2$.

Substituting the above expansions into the original set of equations, and collecting terms of the same orders of ϵ we produce a set of equations. It can be easily seen that in zeroth order in ϵ, we arrive at a steady state problem determining stationary homogeneous solution $\{x_s, y_s\}$. In first order (with $\mathrm{Pe}_1 = 0$) we reproduce the homogeneous linear problem (8) in the form

$$\mathcal{L}\mathbf{u}_1 = (-\partial/\partial t_0 + \mathbf{D}(\mathrm{Pe}_0)\partial^2/\partial \xi_0^2 + \mathbf{V}\partial/\partial \xi_0 + \mathbf{J})\mathbf{u}_1 = 0. \quad (17)$$

Here $\mathbf{D}$ and $\mathbf{V}$ are diffusional and convectional matrices:

$$\mathbf{D}(\mathrm{Pe}) = \begin{pmatrix} 0 & 0 \\ 0 & (\mathrm{Le}\,\mathrm{Pe})^{-1} \end{pmatrix}, \quad \mathbf{V} = \begin{pmatrix} -1 & 0 \\ 0 & -\mathrm{Le}^{-1} \end{pmatrix}.$$

The matrix $\mathbf{J}$ can be found as a Jacobian matrix $\mathbf{F_u}$ of the reaction part of the problem $\mathbf{F}(\mathbf{u}) = \{f(\mathbf{u}), g(\mathbf{u})/\mathrm{Le}\}$ calculated at the stationary point $\mathbf{u}_0$:

$$\mathbf{J} = \begin{pmatrix} -1 - G(y_s) & G'(y_s)H(y_s)/B \\ -B\,G(y_s)/\mathrm{Le} & (G'(y_s)H(y_s) - \alpha)/\mathrm{Le} \end{pmatrix}.$$

The nontrivial solution of the linear problem (17) can be written in the case $\mathrm{Im}\,\sigma = 0$ as

$$\mathbf{u}_1 = a(\xi_1, t_1, t_2, \dots)\mathbf{U}e^{ik_0\xi_0} + \mathrm{c.c.},$$

where $\mathbf{U}$ is the eigenvector corresponding to zero eigenvalue, and a is a complex amplitude of the perturbation, which remains undetermined at this stage. The eigenvector is found as

$$\mathbf{U} = \{G'(y_s)H(y_s)/B, 1 + G(y_s) + ik_0\}.$$

In the next order we arrive at the following inhomogeneous problem:

$$\mathcal{L}\mathbf{u}_2 = \partial\mathbf{u}_1/\partial t_1 - \tfrac{1}{2}\mathbf{F_{uu}}\mathbf{u}_1\mathbf{u}_1. \quad (18)$$

Here $\mathbf{F_{uu}}$ is a tensor of the third rank, with components

$$(F_{\mathbf{uu}})_{ijk} = \frac{\partial^2 \mathbf{F}_i}{\partial \mathbf{u}_j \partial \mathbf{u}_k}$$

and $\mathcal{L}$ is defined in Eq. (17). The solvability condition for Eq. (18) is determined by the orthogonality of a secular part of the inhomogeneity to an eigenvector $\mathbf{U}^\dagger$ of the adjoint linear problem. This vector is given by

$$\mathbf{U}^\dagger = \lambda^{-1}\{-B(1 + G(y_s) - ik_0)/(G'(y_s)H(y_s)\mathrm{Le}), 1\},$$

which satisfies the additional orthogonality condition $(\mathbf{U}^\dagger, \mathbf{U}) = 1$ [$(.,.)$ denotes a scalar product defined as Cartesian scalar product]. Here $\lambda = [(1 + G(y_s))(\mathrm{Le} - 1) + ik_0(\mathrm{Le} + 1)]/\mathrm{Le}$ is the nonzero eigenvalue of the linear problem. It can be easily checked that the solvability condition is equivalent to

$$\partial a/\partial t_1 = 0.$$

The last equation again says nothing about the amplitude behavior in time and space, so we need to proceed to the next order, and to determine part of $\mathbf{u}_2$ orthogonal to $\mathbf{u}_1$. It has two contributions

$$\mathbf{u}_2 = \mathbf{u}_2^{(2)} + \mathbf{u}_2^{(0)},$$

one is proportional to the double spatial frequency mode $\mathbf{u}_2^{(2)}$, and the second corresponds to the constant mode $\mathbf{u}_2^{(0)}$. These contributions are given by

$$\mathbf{u}_2^{(0)} = -\mathbf{F}_\mathbf{u}^{-1}\mathbf{F}_{\mathbf{uu}}\mathbf{U}\mathbf{U}^*|a|^2,$$

$$\mathbf{u}_2^{(2)} = -\frac{1}{2}(\mathbf{F}_\mathbf{u} - 4k_0^2\mathbf{D}(Pe_0) + 2ik_0\mathbf{V})^{-1}\mathbf{F}_{\mathbf{uu}}\mathbf{U}\mathbf{U}a^2,$$

(19)

where * denotes complex conjugation. In the third order in ϵ we obtain the following equation

$$\mathcal{L}\mathbf{u}_3 = \frac{\partial\mathbf{u}_1}{\partial t_2} - \mathbf{D}'(\mathrm{Pe})\frac{\partial^2\mathbf{u}_1}{\partial\xi_0^2}\,\mathrm{Pe}_2 - \left(2\mathbf{D}\frac{\partial}{\partial\xi_0} - \mathbf{V}\right)\frac{\partial\mathbf{u}_1}{\partial\xi_1}$$

$$-\frac{1}{6}\mathbf{F}_{\mathbf{uuu}}\mathbf{u}_1\mathbf{u}_1\mathbf{u}_1 - \mathbf{F}_{\mathbf{uu}}\mathbf{u}_1\mathbf{u}_2. \tag{20}$$

After substitution of Eqs. (19), and projecting on the leading harmonics, we finally arrive at the nontrivial amplitude equation

$$\frac{\partial a}{\partial t_2} = -c_3|a|^2 a + c_1 a + v\frac{\partial a}{\partial\xi_1}. \tag{21}$$

Here the most important cubic term (Landau) coefficient

$$c_3 = 1/2(\mathbf{U}^\dagger, -\mathbf{F}_{\mathbf{uuu}}\mathbf{U}\mathbf{U}\mathbf{U}^* + \mathbf{F}_{\mathbf{uu}}\mathbf{U}^*$$

$$\times(\mathbf{F}_\mathbf{u} - 4k_0^2\mathbf{D}(\mathrm{Pe}_0) + 2ik_0\mathbf{V})^{-1}\mathbf{F}_{\mathbf{uu}}\mathbf{U}\mathbf{U}$$

$$+ 2\mathbf{F}_{\mathbf{uu}}\mathbf{U}\mathbf{F}_\mathbf{u}^{-1}\mathbf{F}_{\mathbf{uu}}\mathbf{U}\mathbf{U}^*). \tag{22}$$

The positive real part of this coefficient corresponds to stable stationary homogeneous amplitude of the Turing-like perturbation. The explicit expression for c_3 is cumbersome, and is omitted here. The linear term coefficient is proportional to the second-order deviation of the bifurcation parameter:

$$c_1 = -k_0^2(\mathbf{U}^\dagger, \mathbf{D}'(\mathrm{Pe}_0)\mathbf{U})\mathrm{Pe}_2.$$

Finally, the convective term coefficient is cast in the form

$$v = (\mathbf{U}^\dagger, (2ik_0\mathbf{D} + \mathbf{V})\mathbf{U}).$$

Substitution of model values for $\mathbf{D}$, $\mathbf{V}$, $\mathbf{U}$, and $\mathbf{U}^\dagger$ produces the following expressions for the above coefficients:

$$c_1 = \frac{k_0^2\mathrm{Le}}{\mathrm{Pe}_0^2\lambda}(1 + G(y_s) + ik_0)\mathrm{Pe}_2,$$

$$v = -\frac{2\mathrm{Le}}{k_0^2\lambda}\left[\frac{k_0^4}{\mathrm{Pe}_0} + ik_0[\alpha(1 + G(y_s)) - G'(y_s)H(y_s)]\right]. \tag{23}$$

The parameter Da can be tuned in order to shift the critical point to the minimum of the neutral curve shown in Fig. 1. The derivation of the amplitude equation in that case is not changed, but the imaginary part of v corresponding to the rate of the perturbation growth $\mathrm{Re}\,\sigma$ vanishes for obvious reasons.

B. Analysis of the amplitude equation

The complex amplitude equation derived in Sec. IV A is valid in an unbounded system, or in a finite length region which is much larger than the length of the critical disturbance. As we show below it can qualitatively describe the behavior of the perturbation amplitude even in a general bounded system with imperfect boundary conditions.

It should be emphasized that the Eq. (21) is actually ill posed; i.e., infinitesimally small perturbations of a solution will grow very fast, so that the original approximation is no longer justified. This feature of Eq. (21) is caused by the fact that in the framework of this equation the linear growth rate $\mathrm{Re}\,\sigma(k)$ is approximated by the linear function of k near the point $k=k_0$. Thus it strongly overestimates the growth rate of the disturbances with $k<k_0$, if $|k-k_0|$ is not small, and leads to a spurious instability of any solutions in an infinite region. Nevertheless, Eq. (21) can be useful in describing solutions which do not contain disturbances with large $|k-k_0|$, e.g., (i) in cases where the spatial modulation of the amplitude is neglected, and thus the wave number prescribed; or (ii) for the calculation of the spatially modulated *steady state* regime where the short-wave modulations which grow fast are excluded from consideration.

It is reasonable to use the polar representation of the complex amplitude $a = re^{i\phi}$, and we arrive at a pair of real equations:

$$\partial r/\partial t_2 = -c_{3r}r^3 + c_{1r}r + v_r\partial r/\partial\xi_1 - v_i r\partial\phi/\partial\xi_1,$$

$$\partial\phi/\partial t_2 = -c_{3i}r^2 + c_{1i} + (v_i/r)\partial r/\partial\xi_1 + v_r\partial\phi/\partial\xi_1. \tag{24}$$

Here the subscripts r and i of the coefficients correspond to the real and imaginary parts of the corresponding quantities.

1. Spatially homogeneous amplitude regime

In this regime ($\partial r/\partial\xi_1 = \partial\phi/\partial\xi_1 = 0$), the equations for the real amplitude r and the phase ϕ are separated. The former equation has a nontrivial stable solution

$$r_s = \sqrt{\frac{c_{1r}}{c_{3r}}}, \tag{25}$$

which is proportional to square root of the parameter's deviation. The solution of the phase equation

$$\phi_s = \frac{c_{3r}c_{1i} - c_{3i}c_{1r}}{c_{3r}}t_2 = \Omega t_2 \tag{26}$$

leads to a frequency shift Ω proportional to the parametric deviation. This implies that the perturbation has the form of a traveling wave with a velocity

$$V = \Omega/k_0. \tag{27}$$
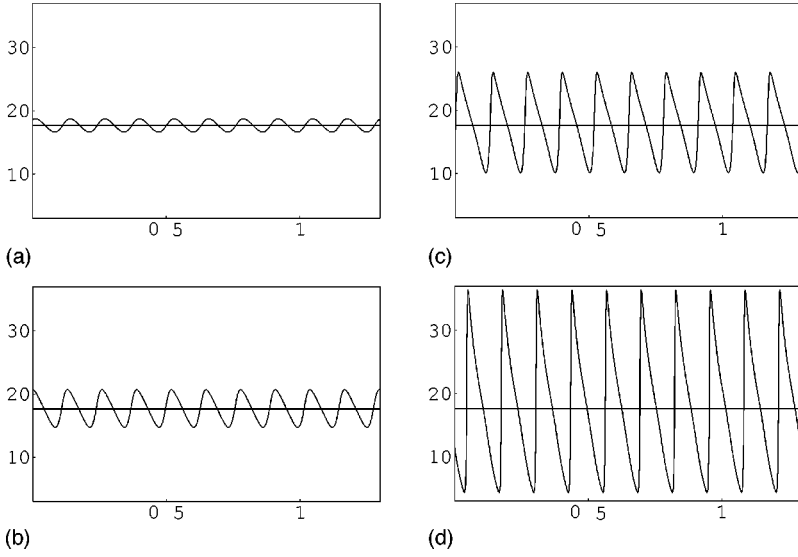
FIG. 2. Snapshots of the temperature profiles for a system with periodic boundary conditions for parameters as in Fig. 1 and $y_s = 17.677$, with varying $Pe > Pe_0 = 98.2$: (a) 102, (b) 110, (c) 200, and (d) 1000. The horizontal lines show the steady state level.

Note that in the case of the infinite region we consider here the nonlinear solution is nonstationary (Hopf bifurcation), though the linear theory predicts a zero frequency at the point $k = k_0$.

2. Spatially modulated stationary regime

Though the amplitude equation (24) is derived for the case of an infinite system or a system with periodic boundary conditions, we are going to check its applicability for the problem in a finite region with realistic boundary condition (4). The achievement of this goal is simplified by the observation that the simulated patterns are stationary (see Sec. V). Let us consider the stationary problem in the semi-infinite regions ($\partial r/\partial t_2 = 0, \partial \phi/\partial t_2 = 0$):

$$dr/d\xi_1 = r(-\tilde{c}_{3r}r^2 + \tilde{c}_{1r}), \quad d\phi/d\xi_1 = (-\tilde{c}_{3i}r^2 + \tilde{c}_{1i})$$
$$(28)$$

($\tilde{c}_3 = -c_3/v$, $\tilde{c}_1 = -c_1/v$), subjected to nonhomogeneous inlet conditions

$$r(0) = r_0, \quad \phi(0) = \phi_0. \tag{29}$$

The solutions of this system are given by

$$r(\xi_1) = \frac{\sqrt{\tilde{c}_{1r}}r_0\exp(\tilde{c}_{1r}\xi_1)}{\sqrt{\tilde{c}_{1r} - \tilde{c}_{3r}r_0^2(1 - \exp(2\tilde{c}_{1r}\xi_1))}},$$
$$(30)$$

$$\phi(\xi_1) = \phi_0 + \tilde{c}_{1i}\xi_1 + \frac{\tilde{c}_{3i}}{2\tilde{c}_{3r}}\ln\frac{\tilde{c}_{1r}}{\tilde{c}_{1r} - \tilde{c}_{3r}r_0^2(1 - \exp(2\tilde{c}_{1r}\xi_1))}.$$

Note that, $\tilde{c}_{1r}$ determines the spatial increment of the amplitude, while $\tilde{c}_{1i}$ gives the wave-number shift. Unfortunately, there is no recipe of converting the original inlet boundary condition (4) into the inlet values r_0, ϕ_0 in Eq. (29) for the amplitude equation (28). We can only fit these values into solution (30) for better agreement with the numerical simulation results. In Sec. V we show that solution (30) of the model system of equations (28) and (29) describes the results of numerical simulations rather well.

Note that the behavior of solution (30) is essentially changed when we cross the amplification threshold $\tilde{c}_{1r} = 0$: negative values of $\tilde{c}_{1r}$ correspond to the nontransparency region, and the positive values to the amplification region. It should be emphasized that the transition described above *is not the Turing bifurcation*. As it was shown in Sec. IV B 1, in the absence of a stationary boundary disturbance the structure excited with $k = k_0$ has a zero frequency only in the limit $Pe \rightarrow Pe_0$, but a nonzero frequency as $Pe > Pe_0$, so that there is a specific case of Hopf bifurcation. Note also that this transition does not correspond to the absolute instability threshold; the latter leads to traveling wave regimes (see, for example, Ref. [20]).

V. NUMERICAL SIMULATIONS

Numerical simulations were conducted around the point of the amplification threshold (Pe_0, k_0) for two different cases. In the first one we choose a set of parameters for which this point coincides with the point of convective instability (Pe_c, k_c), and thus the results of the stability analysis for an unbounded system may by directly applied for the case of a bounded system with periodic boundary conditions. In the following stage we consider the general case when the points of the convective and amplification thresholds are separated, and discuss the emerging patterns and the validity of the analytical predictions derived for an unbounded sys-
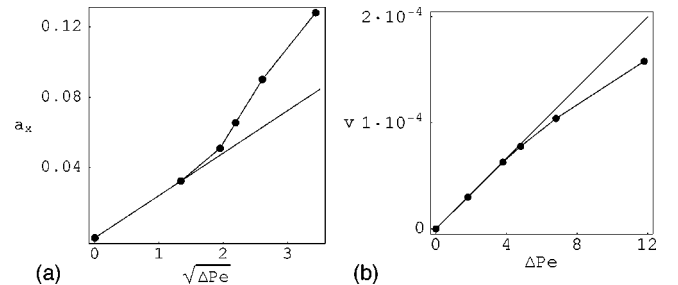
FIG. 3. Comparison of the analytical and numerical dependencies of the perturbation concentration amplitude a_x (a) and the phase wave velocity v (b) on the deviation of the bifurcation parameter ΔPe. Parameters as in Fig. 1, and $y_s = 17.677$.
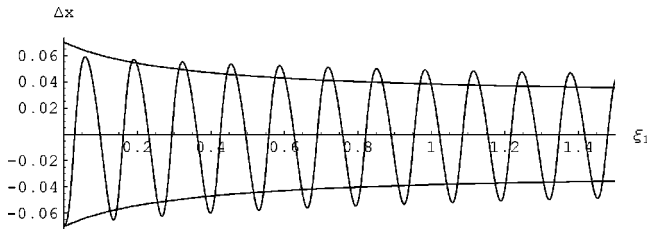
FIG. 4. Comparison of the analytical and numerical dependences of the perturbation concentration amplitude a_x for the boundary condition at the inlet with deviation $\delta\mathbf{u}\sim\mathbf{U}$; Pe$=100$. Parameters as in Fig. 1, and $y_s=17.677$.

tem to a bounded system subject to realistic boundary conditions.

Case 1. The point of amplification threshold is located at the minimum of the neutral curve (for the parameters used in Fig. 1 with $y_s=17.677$; the corresponding critical values are Pe$_c=$Pe$_0=98.2$ and $k_c=k_0=48.47$). For a system with periodic boundary conditions the length of the reactor was chosen to be equal to $L=10(2\pi/k_0)$. Note that the fixed value of L automatically ensures the constant value of k_0, while in the unbounded system this parameter may be affected by the bifurcation parameter. As expected, only the homogeneous solution emerges for Pe$<$Pe$_c=$Pe$_0$. For Pe$>$Pe$_c$ the system exhibits traveling wave solutions with constant amplitudes (Fig. 2). With increasing Pe the form of the profiles changes but the wave number is preserved.

The comparison of numerical and analytical results demonstrates that the value of Pe$_c$ is predicted with a very high accuracy by the linear stability analysis. The concentration amplitude a_x and the velocity of the waves, V, plotted in Fig. 3 as functions of deviations in Pe, can be predicted quite well by nonlinear analysis [Eqs. (25) and (27)] for relatively small ΔPe<5 (the same is valid for the temperature amplitude a_y). For large ΔPe the linearity of the amplitude curves with $\sqrt{\text{Pe}}$ breaks, and the numerical values exceed the theoretical results. The Fourier analysis of the profiles reveals that increasing Pe leads to an excitation of higher harmonics with $k=2k_0$, $k=3k_0$, etc. The impact of these harmonics increases with the Pe number, and leads to a perturbation of the original profile with a single wave number. [It is interesting

to note that the ratio of the amplitudes a_x/a_y, as well as the velocity of the waves V, are in a good agreement with analytical predictions in a relatively large region (ΔPe<10), i.e., the formulas for the eigenvectors may be applied in a wider range of deviation of the bifurcation parameter.]

To elucidate the role of the boundary conditions on the amplitude of the patterns in a bounded systems, we simplified the boundary conditions, using fixed values of the variables at the boundaries $\mathbf{u}|_{\xi=0}=\mathbf{u}_s+\delta\mathbf{u}$ instead of Eq. (4). For deviations $\delta\mathbf{u}\sim\mathbf{U}$, dependences (30) are in a good agreement with numerical results. In the case of arbitrary deviations the phase shift Δk is predicted quite well, but the amplitude behavior can be described only qualitatively (Fig. 4).

Case 2. In the second stage we carried out numerical simulations for Eqs. (3) and (4), for the general case where, in the corresponding unbounded system, the points of amplification threshold and convective instability do not coincide. It should be emphasized that the stability analysis presented above cannot be applied directly for a bounded system (an imperfect bifurcation is expected which is not analyzed in the present investigation). So we study pattern formation by numerical experiments, and test the predictions of the analytical results in the general case.

Typical solutions in a bounded domain (Fig. 5) show that for Pe$<$Pe$_c$ the homogeneous solution (x_s,y_s) is established in most of the domain with some adjustment to the boundary conditions near the inlet section. Note that the critical parameters cannot be determined exactly, but the numerically determined threshold values of Pe for the convective instability and amplification threshold are very closed to the analytical values.

For Pe$>$Pe$_c$ the system exhibits transients of traveling waves: once excited, they move until they are consequently arrested near the boundaries, and finally stationary patterns are formed (the dynamic behavior for Pe$>$Pe$_0$ is illustrated by Fig. 6, but a similar transition takes place for Pe$>$Pe$_c$; see the discussion below). The form of the sustained stationary patterns depends on Pe. In the subcritical region (Pe$<$Pe$_0$), the amplitude of the wavy patterns decays along the reactor, and the profiles $y(z)$ and $x(z)$ tend to the stationary solutions y_s and x_s, similar to the case when Pe$<$Pe$_c$.

For the supercritical conditions (Pe$>$Pe$_0$) stationary pat-
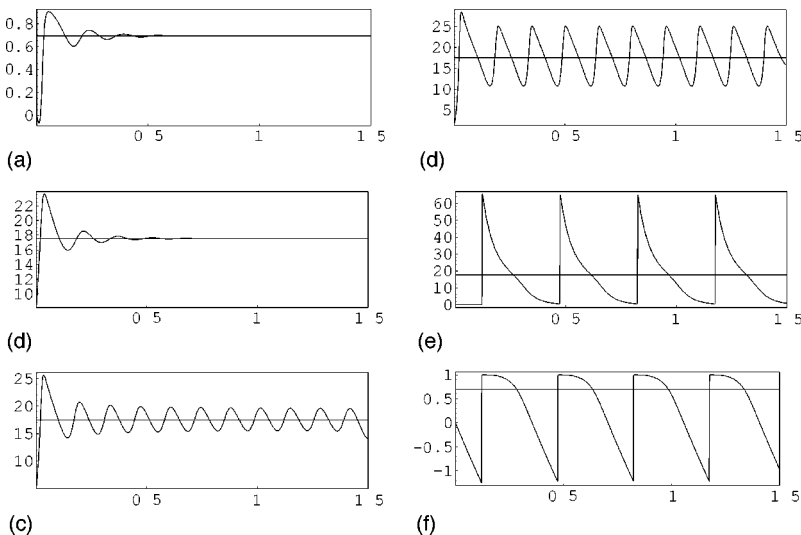
FIG. 5. Steady state profiles in a bounded system with Danckwert's boundary conditions of concentration x [(a) and (f), corresponding to (b) and (e)], and of temperature $y[(b)-(e)]$ for the parameters used in Fig. 1 with varying Pe[(b)Pe$=40<$Pe$_c$, (c) Pe$=60>$Pe$_0$, (d) Pe$=100$, and (e) Pe$=10^4$]. The horizontal lines show the steady state level.
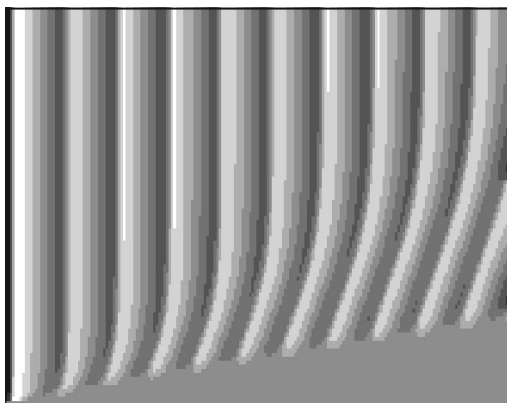
FIG. 6. The transient leading to a sustained pattern starting from a homogeneous state. The temperature is denoted as a grey scale in the time vs space plane. The conditions are as in Fig. 1 with Pe $=100$.

terns are established with an amplitude that varies in space but tends to some saturated value, as follows from the analytical investigation. To the best of our knowledge, such patterns in reaction-convection-diffusion systems were not detected previously. In Ref. [20] moving patterns of similar profiles were detected above the absolute instability threshold in the framework of the complex Ginzburg-Landau equation.

For relatively small deviations $\Delta Pe = Pe - Pe_0$, the patterns have a harmonic form [Fig. 5(c)]. With increasing ΔPe, the amplitude of the state variables increases. This process is accomplished by a transformation of the form of the patterns (similar to case 1), and a decrease of the wave number [see Figs. 5(d) and 5(e)]. Numerical simulations reveal that the form of the patterns becomes insensitive to Pe number for large Pe $(>10^4)$.

The computed wave number is in a very good agreement with the theoretical value k_0 even for large deviations of Pe from the critical value Pe_0, i.e., even when the patterns are not harmonic (the discrepancy does not exceed $\sim 10\%$ for $\Delta Pe \sim Pe_0$). Estimations of the amplitudes based on the critical Pe of the unbound system show that the theory allows us to predict the profile behavior only qualitatively. The poor agreement between numerical results and nonlinear stability predictions in the general case is not surprising, as it takes place even for the degenerate conditions considered in case 1.

VI. CONCLUSION

We study pattern formation in a one-dimensional model of finite-size reactor subject to various types of boundary conditions. This system can be viewed as a particular case of a general reaction-diffusion-convection system which admits one or three homogeneous solutions. The linear stability analysis for this model was performed for the case of an unbounded system, and the analytical expression for amplification threshold was determined. This critical value determines the threshold of the stationary pattern excitation which actually could be sustained in bounded systems. A weak nonlinear analysis was performed for small deviations from the threshold of the general reaction-diffusion-convection problem, and the governing amplitude equation was derived.

The results of linear and nonlinear analyses were verified by direct numerical simulation around two singular points: the oscillatory short-scale (Hopf) bifurcation point for a system with periodic boundary conditions, and the amplification threshold point in a bounded system with Danckwert's boundary conditions. For the first case the critical parameters obtained by the linear stability results for an unbounded system are in very good agreement with numerical results. In the framework of a nonlinear analysis, we determined the velocity of the emerging traveling waves and their amplitude. The boundaries of the applicability of the nonlinear analysis were obtained by a comparison of the amplitude and the velocity dependencies on the bifurcation parameter.

For the second case the numerical results revealed that the sustained stationary patterns are strongly affected by the boundary conditions. The traveling wave patterns corresponding to the convective instability in unbounded systems are effectively dumped by the boundary conditions in a bounded one. The nonuniform *stationary* patterns emerging above the amplification threshold seem to be very similar to *moving* patterns discussed in Ref. [20] in the framework of a complex Ginzburg-Landau equation with nonreflective boundary conditions. Analysis of the latter model, which accounts for both convection and diffusion terms, revealed that mostly convection determines the behavior of the system. Unfortunately, there is no systematic theory that describes the analytical form of boundary conditions for the governing amplitude equation in order to reproduce the numerical results.

Strictly speaking, the linear stability analysis for unbounded systems cannot be applied to bounded system; however, the critical value of the bifurcation parameter can be predicted for relatively small deviations of the boundary conditions from the steady state solution. In this region the nonlinear analysis describes the amplitude envelopes with a very high accuracy. For large deviations of the boundary conditions the critical wave number is still predicted by linear analysis with a very high accuracy; nonlinear analytical results allow one to the resolve the quantitative behavior of the system.

[1] R.J. Deissler, J. Stat. Phys. **40**, 371 (1985).
[2] M.C. Cross, Phys. Rev. Lett. **57**, 2935 (1986).
[3] M.C. Cross and E.Y. Kuo, Physica D **59**, 90 (1992).
[4] A. Couairon and J.M. Chomaz, Physica D **132**, 428 (1999).

[5] P. Manneville, *Dissipative Structure and Weak Turbulence* (Academic Press, Boston, 1990).
[6] M. Sheituch and S. Schvartzman, AIChE. J. **42**, 1041 (1996).
[7] M. Sheintuch and O. Nekhamkina, AIChE. J. **45**, 398 (1999).

[8] Y. Sh. Matros and G.A. Bunimovich, Catal. Rev. Sci. Eng. **38**, 1 (1996).

[9] G. Lauschke and E.D. Gilles, Chem. Eng. Sci. **49**, 5359 (1994).

[10] H. Hua, M. Mangold, A. Kienle, and E.D. Gilles, Chem. Eng. Sci. **53**, 47 (1998).

[11] V.Z. Yakhnin, A.B. Rovinsky, and M. Menzinger, Chem. Eng. Sci. **49**, 3257 (1994).

[12] V.Z. Yakhnin, A.B. Rovinsky, and M. Menzinger, J. Phys. Chem. **98**, 2116 (1994).

[13] V.Z. Yakhnin, A.B. Rovinsky, and M. Menzinger, Chem. Eng. Sci. **50**, 2853 (1995).

[14] M. Sheintuch, O. Lev, S. Mendelbaum, and B. David, Ind. Eng. Chem. Fundam. **25**, 228 (1986).

[15] A. Uppal, W.H. Ray, and A.B. Poore, Chem. Eng. Sci. **29**, 967 (1974).

[16] A. Uppal, W.H. Ray, and A.B. Poore, Chem. Eng. Sci. **31**, 205 (1976).

[17] O. Nekhamkina, B. Rubinstein, and M. Sheintuch (unpublished).

[18] E. M. Lifshits and L. P. Pitaevskii, *Physical Kinetics* (Pergamon, Oxford, 1981).

[19] L.M. Pismen and B.Y. Rubinstein, Int. J. Bifurcation Chaos Appl. Sci. Eng. **9**, 983 (1999).

[20] S.M. Tobias, M.R.E. Proctor, and E. Knobloch, Physica D **113**, 43 (1998).